

Mott-insulator-to-superfluid transition in the Bose-Hubbard model: A strong-coupling approach

K. Sengupta

*Department of Physics, University of Toronto, 60 St. George Street, Toronto, Canada M5T 2Y4 ON
and Department of Physics, Yale University, New Haven, Connecticut 06520-8120, USA*

N. Dupuis

*Department of Mathematics, Imperial College, 180 Queen's Gate, London SW7 2AZ, United Kingdom
and Laboratoire de Physique des Solides, CNRS UMR 8502, Université Paris-Sud, 91405 Orsay, France*

(Received 8 December 2004; published 25 March 2005)

We present a strong-coupling expansion of the Bose-Hubbard model which describes both the superfluid and the Mott phases of ultracold bosonic atoms in an optical lattice. By performing two successive Hubbard-Stratonovich transformations of the intersite hopping term, we derive an effective action which provides a suitable starting point to study the strong-coupling limit of the Bose-Hubbard model. This action can be analyzed by taking into account Gaussian fluctuations about the mean-field approximation as in the Bogoliubov theory of the weakly interacting Bose gas. In the Mott phase, we reproduce results of previous mean-field theories and also calculate the momentum distribution function. In the superfluid phase, we find a gapless spectrum and compare our results with the Bogoliubov theory.

DOI: 10.1103/PhysRevA.71.033629

PACS number(s): 03.75.Lm, 05.30.Jp, 73.43.Nq

I. INTRODUCTION

Recent experiments on ultracold trapped atomic gases have opened a new window onto the phases of quantum matter [1,2]. A gas of bosonic atoms in an optical or magnetic trap has been reversibly tuned between superfluid (SF) and insulating ground states by varying the strength of a periodic potential produced by standing optical waves. This transition has been explained on the basis of the Bose-Hubbard model with on-site repulsive interactions and hopping between nearest-neighbor sites of the lattice [3]. As long as the atom-atom interactions are small compared to the hopping amplitude, the ground state remains superfluid. In the opposite limit of a strong lattice potential, the interaction energy dominates and the ground state is a Mott insulator (MI) when the density is commensurate, with an integer number of atoms localized at each lattice site.

The Gross-Pitaevskii equation or the Bogoliubov theory [4] assume quantum fluctuations to be small and are unable to describe the SF-MI transition and the MI phase. The SF-MI transition is usually studied within a strong-coupling perturbation theory which assumes the kinetic energy to be small and treats exactly the on-site repulsion. In the simplest version, the kinetic energy term is considered within mean-field theory [3,5–7]. The mean-field approximation is well known to give a reasonable estimate of the critical on-site repulsion at which the MI-SF transition occurs. Fluctuation corrections to the mean-field approach have also been considered within a systematic strong-coupling expansion [8]. All these approaches have given a reasonable description of the MI phase and in particular of the excitation spectrum. However, they have not provided a description of the SF phase.

In this work, we develop a strong-coupling expansion of the Bose-Hubbard model which allows us to extend the treatment of Refs. [3,5–7] and describe both the MI and SF phases. Our approach is similar to strong-coupling expan-

sions introduced for the (fermionic) Hubbard model [9,10]. In Sec. II, we derive an effective action for the Bose-Hubbard model in the strong-coupling limit by performing two successive Hubbard-Stratonovich transformations of the intersite hopping term. This effective action involves the exact one- and two-particle Green's functions in the local limit (i.e., in the absence of intersite hopping). We then use the standard Bogoliubov approximation: we perform a saddle-point (or mean-field) approximation and expand the action to quadratic order in the fluctuations (Sec. III). In the MI phase, we recover the previous mean-field result [5,6]: We find a gapped excitation spectrum which becomes gapless at the MI-SF transition. We also calculate the momentum distribution function and study the critical behavior at the transition. In the SF phase, we obtain a gapless spectrum (in agreement with the Goldstone theorem) and compute the Bogoliubov sound mode velocity. We compare our results with the Bogoliubov theory.

II. EFFECTIVE ACTION IN THE STRONG-COUPLING LIMIT

The Bose-Hubbard model is defined by the Hamiltonian

$$H = -t \sum_{\langle \mathbf{r}, \mathbf{r}' \rangle} (\hat{\psi}_{\mathbf{r}}^\dagger \hat{\psi}_{\mathbf{r}'} + \text{H.c.}) - \mu \sum_{\mathbf{r}} \hat{n}_{\mathbf{r}} + \frac{U}{2} \sum_{\mathbf{r}} \hat{n}_{\mathbf{r}}(\hat{n}_{\mathbf{r}} - 1), \quad (1)$$

where $\hat{\psi}_{\mathbf{r}}$, $\hat{\psi}_{\mathbf{r}}^\dagger$ are bosonic operators and $\hat{n}_{\mathbf{r}} = \hat{\psi}_{\mathbf{r}}^\dagger \hat{\psi}_{\mathbf{r}}$. The discrete variable \mathbf{r} labels the different sites (i.e., minima) of the optical lattice. t is the hopping amplitude between nearest sites $\langle \mathbf{r}, \mathbf{r}' \rangle$ and U the on-site repulsion. The optical lattice is assumed to be bipartite with coordination number z . The density, i.e., the average number n of bosons per site, is fixed by the chemical potential μ .

We write the partition function Z as a functional integral over a complex field ψ with the action $S[\psi^*, \psi] = \int_0^\beta d\tau \{ \sum_{\mathbf{r}} \psi_{\mathbf{r}}^* \partial_\tau \psi_{\mathbf{r}} + H[\psi^*, \psi] \}$ (τ is an imaginary time and $\beta = 1/T$ the inverse temperature). Introducing an auxiliary field ϕ to decouple the intersite hopping term by means of a Hubbard-Stratonovich transformation [9,10], we obtain

$$\begin{aligned} Z &= \int \mathcal{D}[\psi^*, \psi, \phi^*, \phi] e^{-(\phi|t^{-1}\phi) + [(\phi|\psi) + \text{c.c.}] - S_0[\psi^*, \psi]} \\ &= Z_0 \int \mathcal{D}[\phi^*, \phi] e^{-(\phi|t^{-1}\phi) \langle e^{(\phi|\psi) + \text{c.c.}} \rangle_0} \\ &= Z_0 \int \mathcal{D}[\phi^*, \phi] e^{-(\phi|t^{-1}\phi) + W[\phi^*, \phi]}, \end{aligned} \quad (2)$$

where we use the shorthand notation $(\phi|\psi) = \sum_a \phi_a^* \psi_a$, $= \int_0^\beta d\tau_a \sum_{\mathbf{r}_a} \phi_a^*(\mathbf{r}_a) \psi(\mathbf{r}_a)$. t^{-1} denotes the inverse of the intersite hopping matrix defined by $t_{\mathbf{r}\mathbf{r}'} = t$ if \mathbf{r}, \mathbf{r}' are nearest neighbors and $t_{\mathbf{r}\mathbf{r}'} = 0$ otherwise. S_0 and Z_0 are the action and partition function in the local limit ($t=0$). $\langle \cdots \rangle_0$ means that the average is taken with $S_0[\psi^*, \psi]$. In the last line of Eq. (2), we have introduced the generating function $W[\phi^*, \phi] = \ln \langle \exp \sum_a (\phi_a^* \psi_a + \text{c.c.}) \rangle_0$ of connected local Green's functions [11],

$$\begin{aligned} G_{\{a_i, b_i\}}^{\text{Rc}} &= (-1)^R \langle \psi_{a_1} \cdots \psi_{a_R} \psi_{b_R}^* \cdots \psi_{b_1}^* \rangle \\ &= \frac{(-1)^R \delta^{(2R)} W[\phi^*, \phi]}{\delta \phi_{a_1}^* \cdots \delta \phi_{a_R}^* \delta \phi_{b_1} \cdots \delta \phi_{b_R}} \Bigg|_{\phi^* = \phi = 0}, \end{aligned} \quad (3)$$

where $\{a_i, b_i\} = \{a_1 \cdots a_R, b_1 \cdots b_R\}$. Inverting Eq. (3), we obtain

$$W[\phi^*, \phi] = \sum_{R=1}^{\infty} \frac{(-1)^R}{(R!)^2} \sum'_{a_1 \cdots b_R} G_{\{a_i, b_i\}}^{\text{Rc}} \phi_{a_1}^* \cdots \phi_{a_R}^* \phi_{b_1} \cdots \phi_{b_R}, \quad (4)$$

where \sum' means that all the fields share the same value of the site index. If we truncate $W[\phi^*, \phi]$ to quartic order in the fields, we obtain the action

$$\begin{aligned} S[\phi^*, \phi] &= (\phi|t^{-1}\phi) - W[\phi^*, \phi] \\ &= \sum_{a,b} \phi_a^* (t_{ab}^{-1} + G_{ab}) \phi_b \\ &\quad - \frac{1}{4} \sum_{a_1, a_2, b_1, b_2} G_{a_1 a_2, b_1 b_2}^{\text{IIc}} \phi_{a_1}^* \phi_{a_2}^* \phi_{b_1} \phi_{b_2}, \end{aligned} \quad (5)$$

where $G \equiv G^I$. Equation (5) was used as a starting point by van Oosten *et al.* to study the instability of the MI with respect to superfluidity [6]. Their results are summarized in Appendix C and lead to the usual mean-field phase diagram shown in Fig. 1. It is tempting to go beyond the mean-field approximation by considering Gaussian fluctuations of the ϕ field about its mean-field value. The Green's function obtained in this way is, however, not physical since it leads in the SF phase to a spectral function which is not normalized to unity [13]. Physical quantities like the excitation spectrum, the velocity of the Bogoliubov sound mode, or the

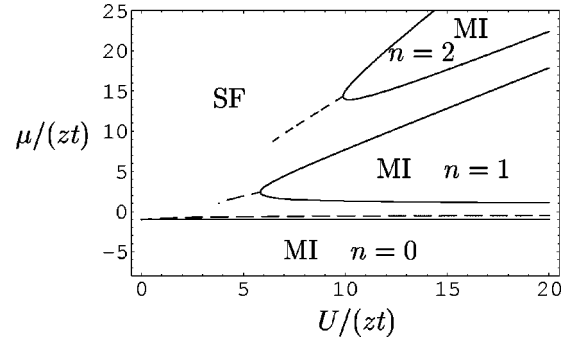


FIG. 1. Phase diagram of the Bose-Hubbard model showing the superfluid (SF) and the Mott insulating (MI) phases at commensurate filling n . The dashed lines correspond to a fixed density $n=0.2$, $n=1$, and $n=2$. For a commensurate density n , the MI-SF transition occurs for $U/(zt) = 2n + 1 + 2(n^2 + n)^{1/2}$ [for $n=1$, this yields $U/(zt) \approx 5.83$, i.e., $U/t \approx 23.31$ for a two-dimensional atomic gas in a square optical lattice].

momentum distribution in the SF phase are therefore out of reach within this approach.

These difficulties can be circumvented if one performs a second Hubbard-Stratonovich decoupling of the hopping term,

$$Z = Z_0 \int \mathcal{D}[\psi^*, \psi, \phi^*, \phi] e^{(\psi|t\psi) - [(\psi|\phi) + \text{c.c.}] + W[\phi^*, \phi]}. \quad (6)$$

In Appendix A, we show that the auxiliary field of this transformation has the same correlation functions as the original boson field (hence the same notation for both fields). The effective action $S[\psi^*, \psi]$ is obtained by integrating out the ϕ field in Eq. (6). This procedure was carried out in detail in Ref. [10] in the context of the fermionic Hubbard model. Similarly, we obtain [12]

$$\begin{aligned} S[\psi^*, \psi] &= - \sum_{a,b} \psi_a^* (G_{ab}^{-1} + t_{ab}) \psi_b \\ &\quad + \frac{1}{4} \sum_{a_1, a_2, b_1, b_2} \Gamma_{a_1 a_2, b_1 b_2}^{\text{II}} \psi_{a_1}^* \psi_{a_2}^* \psi_{b_1} \psi_{b_2}, \end{aligned} \quad (7)$$

where $\Gamma^{\text{II}}(\tau_1, \tau_2; \tau_3, \tau_4)$ is the (exact) two-particle vertex in the local limit. In Eq. (7), we have neglected R -particle vertices ($R \geq 3$) whose amplitudes are given by the (exact) local R -particle vertices Γ^R [10]. Γ^{II} is local in space but has a complicated time dependence (see Appendix B). In the following, we approximate Γ^{II} by its static value (obtained by passing to frequency space and putting all Matsubara frequencies to zero). This approximation is justified for energies much below U where the frequency dependence of the local two-particle vertex is weak. At higher energies, its validity is more difficult to assess. Introducing

$$g = \frac{1}{2} \Gamma^{\text{II}} \Bigg|_{\text{static}}, \quad (8)$$

we finally obtain

$$S = - \int_0^\beta d\tau d\tau' \sum_{\mathbf{r}, \mathbf{r}'} \psi_{\mathbf{r}}^*(\tau) [G^{-1}(\mathbf{r}, \tau; \mathbf{r}', \tau') + t_{\mathbf{r}, \mathbf{r}'} \delta(\tau - \tau')] \psi_{\mathbf{r}'}(\tau') + \frac{g}{2} \int_0^\beta d\tau \sum_{\mathbf{r}} \psi_{\mathbf{r}}^* \psi_{\mathbf{r}} \psi_{\mathbf{r}} \psi_{\mathbf{r}}. \quad (9)$$

The action (9) is the starting point of our analysis. It is analogous to the original action $\int_0^\beta d\tau \sum_{\mathbf{r}} \psi_{\mathbf{r}}^* \partial_\tau \psi_{\mathbf{r}} + H[\psi^*, \psi]$ with two noteworthy differences: the “free” propagator involves the exact local propagator G , and the amplitude of the boson-boson interaction is given by the exact local two-particle vertex (approximated here by its static limit). The action (9) yields the exact partition function $Z = Z_0 \int \mathcal{D}[\psi^*, \psi] e^{-S}$ and the exact Green function $-\langle \psi_{\mathbf{r}}(\tau) \psi_{\mathbf{r}'}^*(\tau') \rangle$ both in the local ($t=0$) and noninteracting ($U=0$) limits [9,10]. By means of two successive Hubbard-Stratonovich transformations of the intersite hopping term, we have thus performed a partial resummation of interaction processes and obtained an effective action which provides a suitable starting point in the strong-coupling limit.

III. MEAN-FIELD AND GAUSSIAN APPROXIMATIONS

In order to study the Mott and superfluid phases from the strong-coupling effective action (9), we use the standard Bogoliubov approximation: we first perform a saddle-point (or mean-field) approximation and then expand the action (9) to quadratic order in the fluctuations. The saddle-point action is given by

$$\frac{S}{N\beta} = -(\bar{G}^{-1} + D)\psi_0^2 + \frac{g}{2}\psi_0^4, \quad (10)$$

where $\bar{G} = (i\omega=0)$, $D = zt$, and N is the total number of lattice sites. The saddle-point value ψ_0 (assumed here, with no loss of generality, to be real) is obtained from $\partial S / \partial \psi_0 = 0$,

$$\psi_0^2 = \begin{cases} \frac{\bar{G}^{-1} + D}{g} & \text{if } \bar{G}^{-1} + D > 0, \\ 0 & \text{otherwise.} \end{cases} \quad (11)$$

The MI-SF therefore occurs when $\bar{G}^{-1} + D = 0$, in agreement with the results of Appendix C, which leads to the phase diagram shown in Fig. 1. Using $\langle \psi_{\mathbf{r}} \rangle = \delta \ln Z(J^*, J) / \delta J_{\mathbf{r}}^*$, where $Z[J^*, J]$ is given by Eq. (A1) of Appendix A, we obtain $\phi_0 = D\psi_0$, where ϕ_0 is the mean value of the auxiliary field. Near the MI-SF transition, where $\bar{G}^{-1} + D \approx 0$, we then find $\phi_0^2 \approx 2(D^{-1} + \bar{G}) / \bar{G}^{1/2}$ in agreement with the result of Appendix C.

To quadratic order in the fluctuations $\tilde{\psi}_{\mathbf{r}} = \psi_{\mathbf{r}} - \psi_0$, we obtain the action

$$S = \frac{1}{2} \sum_{\mathbf{k}, \omega} \left[\tilde{\psi}^*(\mathbf{k}, i\omega), \tilde{\psi}(-\mathbf{k}, -i\omega) \right] \times \begin{pmatrix} -G^{-1}(i\omega) + \epsilon_{\mathbf{k}} + 2g\psi_0^2 & g\psi_0^2 \\ g\psi_0^2 & -G^{-1}(-i\omega) + \epsilon_{-\mathbf{k}} + 2g\psi_0^2 \end{pmatrix} \times \begin{pmatrix} \tilde{\psi}(\mathbf{k}, i\omega) \\ \tilde{\psi}^*(-\mathbf{k}, -i\omega) \end{pmatrix}, \quad (12)$$

where $\tilde{\psi}(\mathbf{k}, i\omega)$ is the Fourier transformed field of $\tilde{\psi}_{\mathbf{r}}(\tau)$ and ω a bosonic Matsubara frequency. $\epsilon_{\mathbf{k}}$, the Fourier transform of $-t_{\mathbf{r}, \mathbf{r}'}$, is the boson dispersion in the absence of the on-site repulsion.

A. Mott phase and the MI-SF transition

In the Mott phase, where $\psi_0=0$, the Green's function $\mathcal{G}(\mathbf{k}, i\omega) = -\langle \psi(\mathbf{k}, i\omega) \psi^*(\mathbf{k}, i\omega) \rangle$ can be directly read off from Eq. (12): $\mathcal{G}^{-1}(\mathbf{k}, i\omega) = G^{-1}(i\omega) - \epsilon_{\mathbf{k}}$. Using Eq. (B2), one obtains

$$\mathcal{G}(\mathbf{k}, i\omega) = \frac{1 - z_{\mathbf{k}}}{i\omega - E_{\mathbf{k}}^-} + \frac{z_{\mathbf{k}}}{i\omega - E_{\mathbf{k}}^+}. \quad (13)$$

The two excitation energies $E_{\mathbf{k}}^\pm$ and the spectral weight $z_{\mathbf{k}}$ are defined by

$$E_{\mathbf{k}}^\pm = -\delta\mu + \frac{\epsilon_{\mathbf{k}}}{2} \pm \frac{1}{2} [\epsilon_{\mathbf{k}}^2 + 4\epsilon_{\mathbf{k}} U_x + U^2]^{1/2},$$

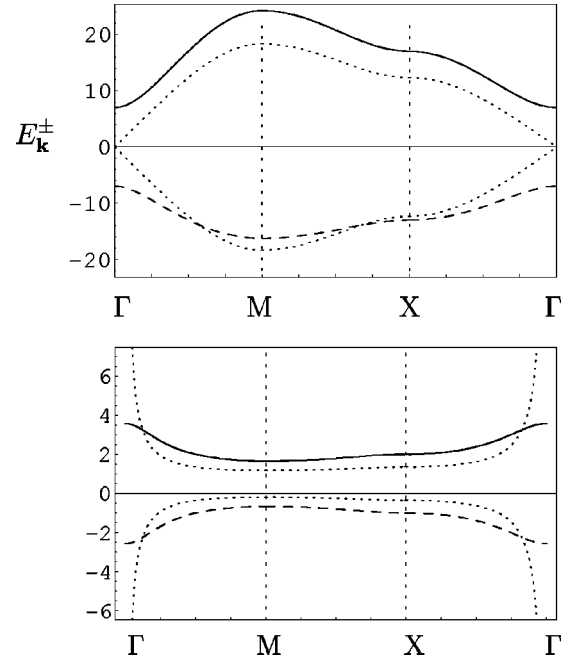
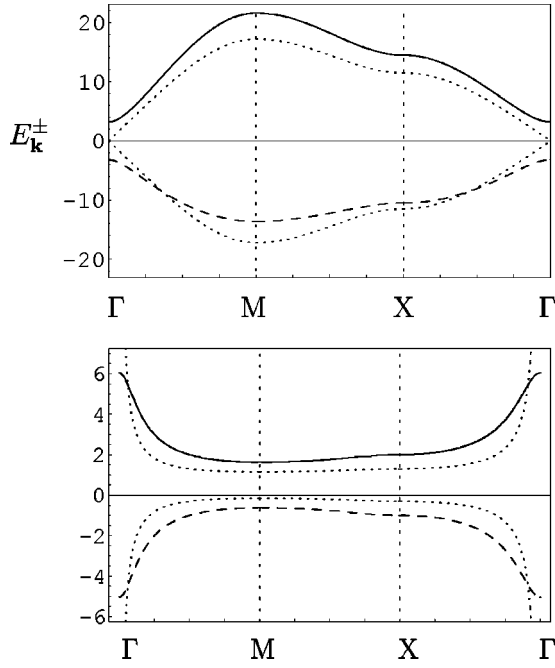


FIG. 2. Top: Excitation energies $E_{\mathbf{k}}^+$ (solid line) and $E_{\mathbf{k}}^-$ (dashed line) in the MI $n=1$ for $U=30t$. Bottom: Spectral weight $z_{\mathbf{k}}$ (solid line) and $1-z_{\mathbf{k}}$ (dashed line). The dotted lines show the result obtained from the Bogoliubov theory (which predicts the phase to be superfluid). [$\Gamma=(0,0)$, $M=(\pi, \pi)$, and $X=(\pi, 0)$.] Results shown in Figs. 2–5 are obtained for a two-dimensional atomic gas in a square optical lattice.


 FIG. 3. Same as Fig. 2, but for $U=25t$.

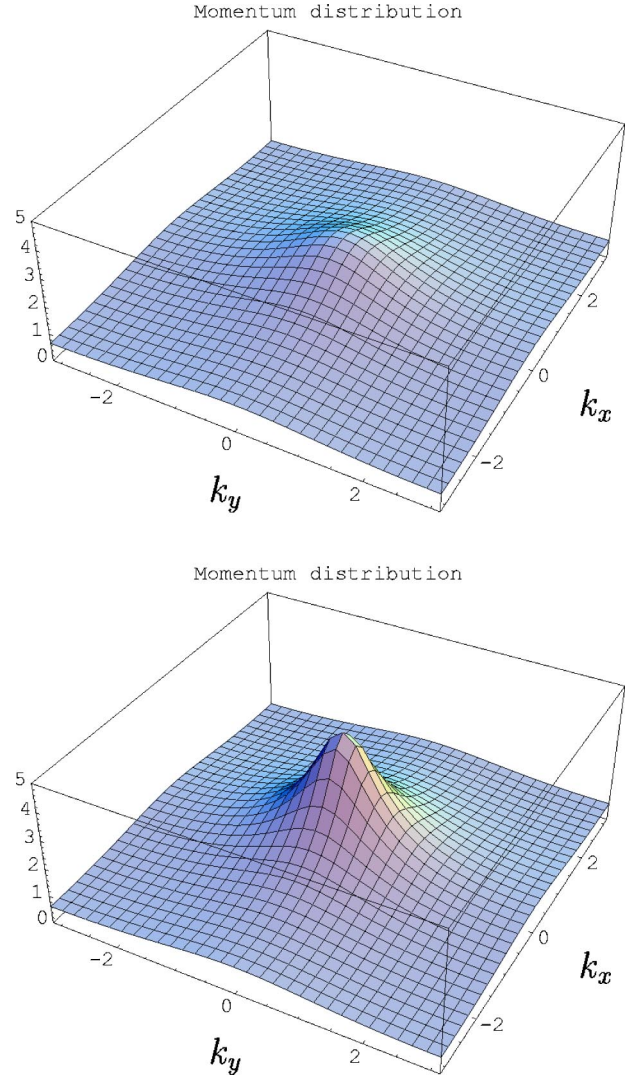
$$z_{\mathbf{k}} = \frac{E_{\mathbf{k}}^+ + \delta\mu + Ux}{E_{\mathbf{k}}^+ - E_{\mathbf{k}}^-}, \quad (14)$$

where $x=n_0+1/2$ and $\delta\mu=\mu-U(n_0-1/2)$. $n_0 \equiv n_0(\mu)$ is the (integer) number of bosons in the local limit for a chemical potential μ (see Appendix B).

The excitation energies $E_{\mathbf{k}}^+, E_{\mathbf{k}}^-$, and the corresponding spectral weight $z_{\mathbf{k}}$ and $1-z_{\mathbf{k}}$, are shown in Figs. 2 and 3 in the MI $n=1$ of a two-dimensional atomic gas in a square optical lattice. The spectrum exhibits a gap $E_{\mathbf{k}=0}^+ - E_{\mathbf{k}=0}^- = (D^2 - 4DUx + U^2)^{1/2}$ which decreases as U decreases. The MI becomes unstable against superfluidity when $E_{\mathbf{k}=0}^+ = 0$ or $E_{\mathbf{k}=0}^- = 0$, which agrees with Eq. (C3) of Appendix C and leads to the phase diagram shown in Fig. 1. The gap $E_{\mathbf{k}=0}^+ - E_{\mathbf{k}=0}^- = (D^2 - 4DUx + U^2)^{1/2}$ closes at the transition if both $E_{\mathbf{k}=0}^+$ and $E_{\mathbf{k}=0}^-$ vanish, which occurs at the tip of the Mott lobe. The MI-SF transition then takes place at fixed density, which is the situation of physical interest. Figures 2 and 3 are obtained with a chemical potential $\delta\mu = -D/2$, which ensures that the MI-SF transition takes place at fixed density $n=1$ (see Appendix C). The decreasing of the Mott gap is accompanied by an increase of spectral weight at $\mathbf{k}=0$, which diverges at the transition. Figures 2 and 3 also show the results of the Bogoliubov theory [as applied to the original Hamiltonian (1)]. The Bogoliubov theory always predicts the ground state to be superfluid [6]. Away from $\mathbf{k}=0$, it provides a good approximation of the negative energy branch $E_{\mathbf{k}}^-$ but gives a poor description of $E_{\mathbf{k}}^+$.

If we expand the equation $E_{\mathbf{k}=0}^\pm = 0$ to order $O(t^2/U)$, we obtain

$$\mu - Un_0 + D(n_0 + 1) + \frac{D^2}{U}(n_0^2 + n_0) = 0,$$


 FIG. 4. Momentum distribution $n_{\mathbf{k}} = \langle \psi_{\mathbf{k}}^* \psi_{\mathbf{k}} \rangle$ in the MI $n=1$ for $U=30t$ (top) and $U=25$ (bottom).

$$\mu - U(n_0 - 1) - Dn_0 - \frac{D^2}{U}(n_0^2 + n_0) = 0, \quad (15)$$

which differs from the energy calculation of Ref. [8] by terms of order $O(t^2/U)$. This discrepancy results from the neglect of the one-loop correction due to Γ^{II} in the calculation of the Green's function [Eq. (13)], which also gives a contribution of order $O(t^2/U)$. However, even without this term the phase diagram looks qualitatively similar to the Freericks and Monien phase diagram.

From the Green's function (13), we can also obtain the momentum distribution $n_{\mathbf{k}} = \langle \psi_{\mathbf{k}}^* \psi_{\mathbf{k}} \rangle = -\int_{-\infty}^0 d\omega A(\mathbf{k}, \omega) = 1 - z_{\mathbf{k}}$. $n_{\mathbf{k}}$ measures the spectral weight of the negative energy $E_{\mathbf{k}}^-$ of the spectrum. Deep in the Mott phase, the momentum distribution is roughly flat. Closer to the MI-SF transition, a peak develops around $\mathbf{k}=0$. This peak diverges at the transition (Fig. 4).

The critical theory of the SF-MI transition can be obtained from the action (9) by expanding the inverse propagator $G^{-1}(i\omega) - \epsilon_{\mathbf{k}}$ to quadratic order in \mathbf{k} and ω . Noting that

$\partial G^{-1}(i\omega)/\partial(i\omega)|_{i\omega=0} = \partial \bar{G}^{-1}/\partial \mu$ (and similarly for the second-order derivative), we obtain

$$S = \int_0^\beta d\tau \int dr \left[r_0 |\psi_{\mathbf{r}}|^2 + K_1 \psi_{\mathbf{r}}^* \partial_\tau \psi_{\mathbf{r}} + K_2 |\partial_\tau \psi_{\mathbf{r}}|^2 + K_3 |\nabla \psi_{\mathbf{r}}|^2 + \frac{u}{2} |\psi_{\mathbf{r}}|^4 \right], \quad (16)$$

where

$$r_0 \propto \bar{G}^{-1} + D, \quad (17)$$

$$K_1 \propto \frac{\partial r_0}{\partial \mu}.$$

At all points on the MI-SF transition line except at the Mott lob tip, r_0 vanishes but K_1 remains finite. The critical theory has then a dynamical exponent $z=2$. At the tip of the Mott lob where both r_0 and K_1 vanish, the dynamical exponent $z=1$. A similar analysis, based on the effective action $S[\phi^*, \phi]$, can be found in Ref. [7].

B. Superfluid phase

In the SF phase ($\psi_0 \neq 0$), the Green's function of the $\tilde{\psi}$ field is obtained by inverting the 2×2 matrix propagator in Eq. (12). For the diagonal component $\mathcal{G}(\mathbf{k}, i\omega) = -\langle \tilde{\psi}(\mathbf{k}, i\omega) \tilde{\psi}^*(\mathbf{k}, i\omega) \rangle$, we obtain

$$\mathcal{G}(\mathbf{k}, i\omega) = \frac{(i\omega + \delta\mu + Ux)(i\omega - z_{\mathbf{k}}^+)(i\omega - z_{\mathbf{k}}^-)}{(\omega^2 + E_{\mathbf{k}}^{+2})(\omega^2 + E_{\mathbf{k}}^{-2})}, \quad (18)$$

where

$$E_{\mathbf{k}}^{\pm 2} = -\frac{B_{\mathbf{k}}}{2} \pm \frac{1}{2}(B_{\mathbf{k}}^2 - 4C_{\mathbf{k}})^{1/2},$$

$$z_{\mathbf{k}}^{\pm} = \frac{\tilde{A}_{\mathbf{k}}}{2} \pm \frac{1}{2}(\tilde{A}_{\mathbf{k}}^2 - 4\tilde{B}_{\mathbf{k}})^{1/2},$$

$$\tilde{A}_{\mathbf{k}} = 2\delta\mu - 2(\bar{G}^{-1} + D) - \epsilon_{\mathbf{k}},$$

$$\tilde{B}_{\mathbf{k}} = -(2\bar{G}^{-1} + 2D + \epsilon_{\mathbf{k}})(\delta\mu + Ux) + \delta\mu^2 - \frac{U^2}{4},$$

$$B_{\mathbf{k}} = 2\tilde{B}_{\mathbf{k}} - \tilde{A}_{\mathbf{k}}^2 + (\bar{G}^{-1} + D)^2,$$

$$C_{\mathbf{k}} = \tilde{B}_{\mathbf{k}}^2 - (\bar{G}^{-1} + D)^2(\delta\mu + Ux)^2. \quad (19)$$

From Eq. (18), we deduce the spectral function $A(\mathbf{k}, \omega) = -(1/\pi) \text{Im} \mathcal{G}(\mathbf{k}, \omega + i0^+)$,

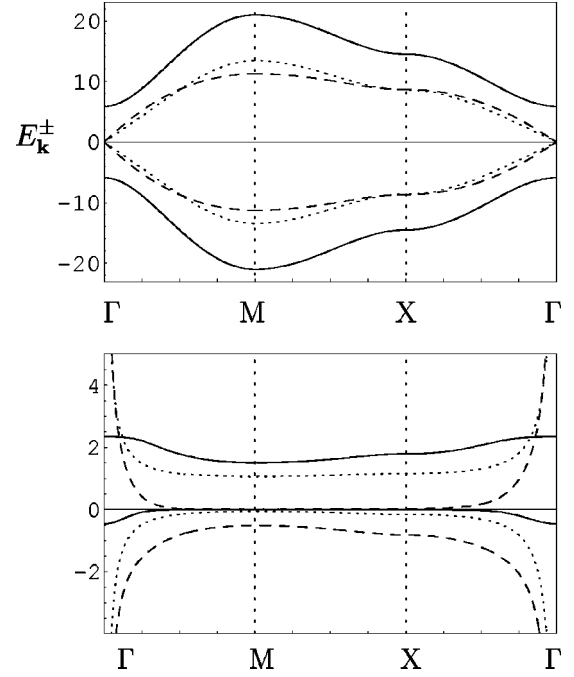


FIG. 5. Excitation energies $\pm E_{\mathbf{k}}^{\pm}$ and spectral weight in the SF phase $n=1$ and $U=20$.

$$A(\mathbf{k}, \omega) = \frac{(E_{\mathbf{k}}^+ + \delta\mu + Ux)(E_{\mathbf{k}}^+ - z_{\mathbf{k}}^+)(E_{\mathbf{k}}^+ - z_{\mathbf{k}}^-)}{2E_{\mathbf{k}}^+(E_{\mathbf{k}}^{+2} - E_{\mathbf{k}}^{-2})} \delta(\omega - E_{\mathbf{k}}^+) + \frac{(E_{\mathbf{k}}^+ - \delta\mu - Ux)(E_{\mathbf{k}}^+ + z_{\mathbf{k}}^+)(E_{\mathbf{k}}^+ + z_{\mathbf{k}}^-)}{2E_{\mathbf{k}}^+(E_{\mathbf{k}}^{+2} - E_{\mathbf{k}}^{-2})} \delta(\omega + E_{\mathbf{k}}^+) - \frac{(E_{\mathbf{k}}^- + \delta\mu + Ux)(E_{\mathbf{k}}^- - z_{\mathbf{k}}^+)(E_{\mathbf{k}}^- - z_{\mathbf{k}}^-)}{2E_{\mathbf{k}}^-(E_{\mathbf{k}}^{+2} - E_{\mathbf{k}}^{-2})} \delta(\omega - E_{\mathbf{k}}^-) - \frac{(E_{\mathbf{k}}^- - \delta\mu - Ux)(E_{\mathbf{k}}^- + z_{\mathbf{k}}^+)(E_{\mathbf{k}}^- + z_{\mathbf{k}}^-)}{2E_{\mathbf{k}}^-(E_{\mathbf{k}}^{+2} - E_{\mathbf{k}}^{-2})} \delta(\omega + E_{\mathbf{k}}^-). \quad (20)$$

The Green's function (18) has the desired physical properties. The spectral function is normalized, $\int_{-\infty}^{\infty} d\omega A(\mathbf{k}, \omega) = 1$, and has the correct sign: $\text{sgn}[A(\mathbf{k}, \omega)] = \text{sgn}(\omega)$ [13]. There are four excitation branches $\pm E_{\mathbf{k}}^{\pm}$, two of which ($\pm E_{\mathbf{k}}^-$) are gapless for $\mathbf{k} \rightarrow \mathbf{0}$ (Fig. 5). However, for a given value of \mathbf{k} , only two branches carry a significant spectral weight. Away from $\mathbf{k} = \mathbf{0}$, the spectral weight is almost completely exhausted by $E_{\mathbf{k}}^+$ and $-E_{\mathbf{k}}^-$. In the vicinity of $\mathbf{k} = \mathbf{0}$, the two gapless branches $\pm E_{\mathbf{k}}^-$ exhaust the spectral weight. By expanding $E_{\mathbf{k}}^-$ in the vicinity of $\mathbf{k} \rightarrow \mathbf{0}$, we find a linear spectrum

$$E_{\mathbf{k}}^- = c|\mathbf{k}|, \quad (21)$$

where

$$c = \left[\frac{2t(\bar{G}^{-1} + D)}{\alpha^2 + 2\gamma(\bar{G}^{-1} + D)} \right]^{1/2},$$

$$\alpha = \frac{\delta\mu^2 + 2\delta\mu Ux + U^2/4}{(\delta\mu + Ux)^2},$$

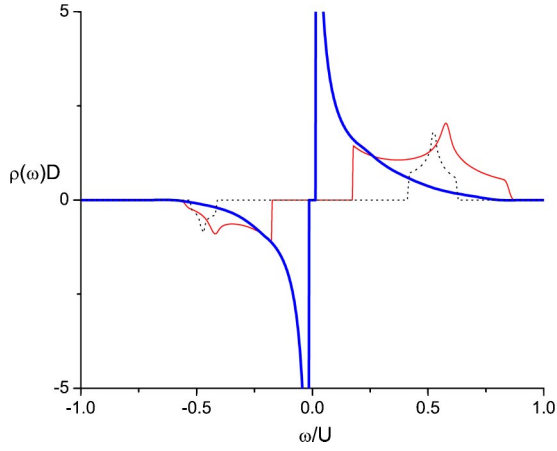


FIG. 6. Integrated spectral function $\rho(\omega) = \int [d^2k / (2\pi)^2] A(\mathbf{k}, \omega)$ in the MI $n=1$ ($\mu = U/2 - D/2$): $U/t=80$ (dashed line), 40 (thin solid line), and 23.33 (thick solid line). The transition to the SF phase occurs for $U/t \approx 23.31$.

$$\gamma = \frac{U^2(x^2 - 1/4)}{(\delta\mu + Ux)^3}. \quad (22)$$

Our strong-coupling approach therefore reproduces the Bogoliubov (Goldstone) mode of the SF phase.

As discussed in Sec. III A, our strong-coupling theory is not an expansion order by order in t/U . For this reason, the computation of the chemical potential from the single-particle Green's function, i.e., $n = \text{Tr}(\mathcal{G})$, is not reliable. We have therefore used the chemical potential obtained within the mean-field approximation discussed in Appendix C.

Figure 5 also shows the results of the Bogoliubov theory [as applied to the Hamiltonian (1)] for the *same* chemical potential μ . The Bogoliubov theory provides a good approximation to $E_{\mathbf{k}}^-$ and therefore to the low-energy part of the excitation spectrum. This implies that the velocity of the gapless mode [Eq. (22)] can be approximated by the Bogoliubov result $c = [2t(\mu + D)]^{1/2}$. Away from $\mathbf{k} = \mathbf{0}$, the Bogoliubov approach gives a rather poor description of $E_{\mathbf{k}}^+$.

The Green's function $\mathcal{G}(\mathbf{k}, i\omega)$ yields the momentum distribution

$$n_{\mathbf{k}} = \langle \psi_{\mathbf{k}}^* \psi_{\mathbf{k}} \rangle = N \psi_0^2 \delta_{\mathbf{k},0} - \int_{-\infty}^0 d\omega A(\mathbf{k}, \omega). \quad (23)$$

Apart from the condensate contribution $N \psi_0^2 \delta_{\mathbf{k},0}$, the momentum distribution function is directly given by the spectral weight of the negative energies $-E_{\mathbf{k}}^+$ and $-E_{\mathbf{k}}^-$ (Fig. 5).

Figure 6 shows the integrated spectral function $\rho(\omega) = \int [d^2k / (2\pi)^2] A(\mathbf{k}, \omega)$ for a commensurate density $n=1$. Deep in the Mott phase, $\rho(\omega)$ is essentially given by the noninteraction density of states of free bosons on the square lattice centered around $-\mu$ and $U-\mu$ and with relative spectral weights $-n_0$ and n_0+1 . The two peaks near $\omega = -\mu$ and $\omega = U-\mu$ are due to the Van Hove singularities in the density of states of free bosons. When decreasing the value of U/t , the Mott gap decreases and $\rho(\omega)$ strongly increases at the

gap edges. At the critical value $U/t \approx 23.31$, the gap closes and $\rho(\omega)$ diverges at $\omega=0$. This divergence persists in the superfluid phase.

IV. CONCLUSION

By performing two successive Hubbard-Stratonovich transformations of the intersite hopping term, we have shown how to derive an effective action which provides a suitable starting point to study the strong-coupling limit of the Bose-Hubbard model. This action can then be analyzed by taking into account Gaussian fluctuations about the mean-field approximation as in the Bogoliubov theory of the weakly interacting Bose gas. The main improvement over previous related approaches [5–8] is the possibility to describe both the Mott and SF phases. Both in the Mott and SF phases, we compute the excitation spectrum and the momentum distribution. Our approach clearly shows how the excitation spectrum, which is gapped in the MI phase, becomes gapless at the MI-SF transition.

The strong-coupling expansion presented in this paper should in principle also apply to more complicated situations where, for instance, several atom species are present in the optical lattice.

Note added. Recently, we became aware of two related works. Konabe *et al.* [14] have studied the single-particle excitation spectrum in the Mott phase and obtained results similar to ours. The method used by these authors bears some similarities with the strong-coupling expansion discussed in the present paper. Within a slave-boson representation of the Bose-Hubbard model, Dickerscheid *et al.* [15] have discussed both the Mott and SF phases. Their results agree with ours (whenever the comparison is possible).

APPENDIX A: HUBBARD-STRATONOVICH TRANSFORMATIONS

The Green's functions of the boson field ψ can be obtained from the generating function [11]

$$Z[J^*, J] = \int \mathcal{D}[\psi^*, \psi] e^{(\psi | t \psi) - S_0[\psi^*, \psi] + [(J | \psi) + \text{c.c.}]}, \quad (A1)$$

where $J_{\mathbf{r}}^*$, $J_{\mathbf{r}}$ are external sources. After the Hubbard-Stratonovich decoupling of the intersite hopping term [see Eq. (2)] and the shift $\phi^* \rightarrow \phi^* - J^*$, $\phi \rightarrow \phi - J$ of the auxiliary field, we obtain

$$\begin{aligned} Z[J^*, J] &= \int \mathcal{D}[\psi^*, \psi, \phi^*, \phi] e^{-(\phi - J | t^{-1}(\phi - J)) + [(\phi | \psi) + \text{c.c.}] - S_0[\psi^*, \psi]} \\ &= Z_0 \int \mathcal{D}[\phi^*, \phi] e^{-(\phi - J | t^{-1}(\phi - J)) + W[\phi^*, \phi]}. \end{aligned} \quad (A2)$$

A second Hubbard-Stratonovich decoupling of the hopping term (with an auxiliary field ψ') leads to

$$\begin{aligned}
Z[J^*, J] &= Z_0 \int \mathcal{D}[\psi'^*, \psi', \phi^*, \phi] e^{(\psi' | t \psi') - [(\psi' | \phi - J) + \text{c.c.}] + W[\phi^*, \phi]} \\
&= Z_0 \int \mathcal{D}[\psi'^*, \psi', \phi^*, \phi] \\
&\quad \times e^{(\psi' | t \psi') - [(\psi' | \phi) + \text{c.c.}] + [(\psi' | J) + \text{c.c.}] + W[\phi^*, \phi]}. \quad (\text{A3})
\end{aligned}$$

From Eq. (A3) we deduce that $Z[J^*, J]$ is also the generating function of the Green's functions of the ψ' field. ψ' can therefore be identified with the original boson field ψ .

APPENDIX B: CALCULATION OF THE LOCAL GREEN'S FUNCTIONS G and G^{II}

In the absence of intersite hopping ($t=0$), the states $|p\rangle = (p!)^{-1/2} (\hat{\psi}^\dagger)^p |0\rangle$ ($p \geq 0$ integer) are eigenstates with eigenvalues $\epsilon_p = -\mu p + (U/2)p(p-1)$. (We consider a single site and therefore drop the site index.) $|0\rangle$ is the vacuum of particles. This yields the partition function $Z_0 = \sum_{p=0}^{\infty} e^{-\beta \epsilon_p}$. In the ground state, for a given value of the chemical potential μ ,

there are n_0 bosons per site, where n_0 is obtained from $\epsilon_{n_0} = \min_p \epsilon_p$. The latter condition leads to $n_0 - 1 \leq \mu/U \leq n_0$ if $\mu \geq -U$, and $n_0 = 0$ if $\mu \leq -U$. Note that n_0 is integer (except when $\mu/U = p$ is integer; the states $|p\rangle$ and $|p+1\rangle$ are then degenerate), even when the boson density n is not.

The single-particle Green's function $G(\tau) = -\langle T_\tau \hat{\psi}(\tau) \hat{\psi}^\dagger(0) \rangle$ is easily calculated using the closure relation $\sum_{p=0}^{\infty} |p\rangle \langle p| = 1$. For $\tau > 0$, one finds

$$G(\tau) = -\frac{1}{Z_0} \sum_{p=0}^{\infty} (p+1) e^{-(\beta-\tau)\epsilon_p - \tau\epsilon_{p+1}}, \quad (\text{B1})$$

and, in frequency space,

$$G(i\omega) = \frac{-n_0}{i\omega + \epsilon_{n_0-1} - \epsilon_{n_0}} + \frac{n_0 + 1}{i\omega + \epsilon_{n_0} - \epsilon_{n_0+1}}, \quad (\text{B2})$$

where ω is a bosonic Matsubara frequency.

The two-particle Green's function can be calculated in the same way. One finds

$$\begin{aligned}
G^{\text{II}}(\tau_1, \tau_2; \tau_3, \tau_4 = 0) &= \langle T_\tau \hat{\psi}(\tau_1) \hat{\psi}(\tau_2) \hat{\psi}^\dagger(0) \hat{\psi}^\dagger(\tau_3) \rangle = \frac{1}{Z_0} \sum_{p=0}^{\infty} e^{-\beta \epsilon_p} \{ (p+1)(p+2) e^{\tau_1(\epsilon_p - \epsilon_{p+1}) + \tau_2(\epsilon_{p+1} - \epsilon_{p+2}) + \tau_3(\epsilon_{p+2} - \epsilon_{p+1})} \\
&\quad \times \theta(\tau_1 - \tau_2) \theta(\tau_2 - \tau_3) + (p+1)(p+2) e^{\tau_1(\epsilon_{p+1} - \epsilon_{p+2}) + \tau_2(\epsilon_p - \epsilon_{p+1}) + \tau_3(\epsilon_{p+2} - \epsilon_{p+1})} \theta(\tau_2 - \tau_1) \theta(\tau_1 - \tau_3) \\
&\quad + (p+1)^2 e^{\tau_1(\epsilon_p - \epsilon_{p+1}) + \tau_2(\epsilon_p - \epsilon_{p+1}) + \tau_3(\epsilon_{p+1} - \epsilon_p)} [\theta(\tau_1 - \tau_3) \theta(\tau_3 - \tau_2) + \theta(\tau_2 - \tau_3) \theta(\tau_3 - \tau_1)] \\
&\quad + p(p+1) e^{\tau_1(\epsilon_{p-1} - \epsilon_p) + \tau_2(\epsilon_p - \epsilon_{p+1}) + \tau_3(\epsilon_p - \epsilon_{p-1})} \theta(\tau_3 - \tau_1) \theta(\tau_1 - \tau_2) \\
&\quad + p(p+1) e^{\tau_1(\epsilon_p - \epsilon_{p+1}) + \tau_2(\epsilon_{p-1} - \epsilon_p) + \tau_3(\epsilon_p - \epsilon_{p-1})} \theta(\tau_3 - \tau_2) \theta(\tau_2 - \tau_1) \}. \quad (\text{B3})
\end{aligned}$$

After a somewhat tedious calculation, we obtain for the Fourier transform of the connected part in the static limit

$$\begin{aligned}
\bar{G}^{\text{IIc}} &= \int_0^\beta d\tau_1 d\tau_2 d\tau_3 G^{\text{II}}(\tau_1, \tau_2; \tau_3, 0) - 2\beta [G(i\omega = 0)]^2 \\
&= -\frac{4(n_0+1)(n_0+2)}{[2\mu - (2n_0+1)U](Un_0 - \mu)^2} - \frac{4n_0(n_0-1)}{[\mu - U(n_0-1)]^2 [U(2n_0-3) - 2\mu]} + \frac{4n_0(n_0+1)}{(\mu - Un_0)[- \mu + U(n_0-1)]^2} \\
&\quad + \frac{4n_0(n_0+1)}{(\mu - Un_0)^2 [- \mu + U(n_0-1)]} + \frac{4n_0^2}{[- \mu + U(n_0-1)]^3} + \frac{4(n_0+1)^2}{(\mu - Un_0)^3}. \quad (\text{B4})
\end{aligned}$$

The static limit of the two-particle vertex Γ^{II} is equal to $-\bar{G}^{\text{IIc}}/\bar{G}^4$.

APPENDIX C: AUXILIARY-FIELD MEAN-FIELD APPROACH

In this appendix, we review the mean-field results obtained from the action $S[\phi^*, \phi]$ [Eq. (5)] [6]. Within a saddle-point approximation, where the field ϕ_0 is taken real and assumed to be time- and space-independent, the action becomes

$$\frac{S}{N\beta} = (D^{-1} + \bar{G})\phi_0^2 - \frac{1}{4}\bar{G}^{\text{IIc}}\phi_0^4, \quad (\text{C1})$$

where $D = zt$. \bar{G} and \bar{G}^{IIc} are the single-particle and two-particle local Green's functions in the static limit (see Appendix B). The ground-state energy per site $E = -\lim_{\beta \rightarrow \infty} (1/N\beta) \ln Z$ is then given by [see Eq. (2)]

$$E = a_0 + a_2\phi_0^2 + a_4\phi_0^4, \quad (\text{C2})$$

where $a_0 = -\lim_{\beta \rightarrow \infty} (1/N\beta) \ln Z_0$ is the ground-state energy in the local limit, $a_2 = D^{-1} + \bar{G}$, and $a_4 = -(1/4)\bar{G}^{\text{IIc}}$. The mean-

field value ϕ_0 is obtained by minimizing E . ϕ_0 vanishes in the Mott phase ($a_2 > 0$) and takes a finite value in the SF phase ($a_2 < 0$). The MI-SF transition is then given by $a_2 = 0$, which leads to

$$\delta\mu_{\pm} = -\frac{D}{2} \pm \frac{1}{2}[D^2 + U^2 - 4DUx]^{1/2}, \quad (\text{C3})$$

where n_0 is the integer number of bosons in the local limit for a chemical potential μ (see Appendix B). x and $\delta\mu$ are defined in Sec. III. For each value of n_0 , Eq. (C3) defines a Mott lobe in the U - μ phase diagram (Fig. 1), whose tip corresponds to $\delta\mu_+ = \delta\mu_- = -zt/2$ and $U/(zt) = 2n_0 + 1 + 2(n_0^2 + n_0)^{1/2}$. At the lobe tip, $\partial a_2 / \partial \mu = 0$.

In the SF phase, the order parameter ϕ_0 is given by $\phi_0^2 = -a_2/(2a_4)$, and the ground-state energy takes the value

$$E = a_0 - \frac{a_2^2}{4a_4}. \quad (\text{C4})$$

From Eq. (C4), we deduce the mean boson density

$$n = -\frac{\partial E}{\partial \mu} = n_0 + \frac{1}{4} \frac{\partial}{\partial \mu} \left(\frac{a_2^2}{a_4} \right) \simeq n_0 + \frac{a_2}{2a_4} \frac{\partial a_2}{\partial \mu}, \quad (\text{C5})$$

where the last equality holds near the MI-SF transition ($a_2 \approx 0$). We have used $n_0 = -\partial a_0 / \partial \mu$. We conclude that, at the MI-SF transition, the boson density remains pinned at the integer value n_0 if $\partial a_2 / \partial \mu = 0$, which corresponds to the tip of the Mott lobe in the μ - U phase diagram (Fig. 1).

-
- [1] M. Greiner, O. Mandel, T. Esslinger, T. W. Hänsch, and I. Bloch, *Nature (London)* **415**, 39 (2002).
- [2] T. Stöferle, H. Moritz, C. Schori, M. Köhl, and T. Esslinger, *Phys. Rev. Lett.* **92**, 130401 (2004).
- [3] M. P. A. Fisher, P. B. Weichman, G. Grinstein, and D. S. Fisher, *Phys. Rev. B* **40**, 546 (1989); D. Jaksch, C. Bruder, J. I. Cirac, C. W. Gardiner, and P. Zoller, *Phys. Rev. Lett.* **81**, 3108 (1998).
- [4] See, for instance, L. Pitaevskii and S. Stringari, *Bose-Einstein Condensation* (Oxford University Press, Oxford, 2003).
- [5] K. Sheshadri, H. R. Krishnamurthy, R. Pandit, and T. V. Ramakrishnan, *Europhys. Lett.* **22**, 257 (1993).
- [6] D. Van Oosten, P. van der Straten, and H. T. C. Stoof, *Phys. Rev. A* **63**, 053601 (2001).
- [7] S. Sachdev, *Quantum Phase Transitions* (Cambridge University press, Cambridge, England, 1999).
- [8] J. K. Freericks and H. Monien, *Europhys. Lett.* **26**, 545 (1994); *Phys. Rev. B* **53**, 2691 (1996).
- [9] S. Pairault, D. Sénéchal, and A.-M. S. Tremblay, *Phys. Rev. Lett.* **80**, 5389 (1998); *Eur. Phys. J. B* **16**, 85 (2000).
- [10] N. Dupuis, *Nucl. Phys. B* **617**, 618 (2000); e-print cond-mat/0105063.
- [11] See, for instance, J. W. Negele and H. Orland, *Quantum Many Particle Systems* (Addison-Wesley, Reading, MA, 1988).
- [12] Here we neglect the ‘‘anomalous’’ terms of the action since they play no role in the following [10].
- [13] As noted by Pairault *et al.* [9], strong-coupling expansions usually lead to a nonphysical single-particle Green’s function (e.g., a negative spectral weight in fermion systems or a non-normalized spectral function).
- [14] S. Konabe, T. Nikuni, and M. Nakamura, e-print cond-mat/0407229.
- [15] D. B. M. Dickerscheid, D. van Oosten, P. J. H. Denteneer, and H. J. Stoof, *Phys. Rev. A* **68**, 043623 (2003).